Desalination and Water Treatment
www.deswater.com
20 (2010) 102–113
August
1944-3994 / 1944-3986 © 2010 Desalination Publications. All rights reserved.
doi: 10.5004/dwt.2010.1215

Removal of reactive dye from aqueous solutions by adsorption onto activated carbons prepared from oak sawdust

Mona Mahmoud Abd El-Latif[a]*, Amal Mozarei Ibrahim[b]

[a]*Fabrication Technology Department, Institute of Advanced Technologies and New Materials, Mubarak City for Scientific Research and Technology Applications, P.O. Box 21934, Alexandria, Egypt*
Tel.+20 (3) 4593414; Fax +20 (3) 4593414; email: amona1911@yahoo.com
[b]*Surface Chemistry and Catalysis Laboratory, Physical Chemistry Department, National Research Center, El-Tahrir St., Dokki, Cairo, Egypt*
Tel. +20 (2) 3335977; Fax +20 (2) 3370931; email: amozarei@yahoo.com

Received 19 May 2009; Accepted in revised form 11 January 2010

ABSTRACT

Activated carbons prepared from oak sawdust, a timber industry waste, have been examined for the removal of remazol brilliant blue (RB) dye from aqueous solutions through batch adsorption technique. Activated carbons were prepared from oak sawdust by chemical activation with 10% HNO_3 (AC1) followed by pyrolysis at 500°C in the absence of air and by physical activation at 500°C in the absence of air (AC2). Activated carbons were characterized by SEM, BET and FTIR. Also pH_{pzc} was followed by pyrolysis at 500°C in the absence of air and by physical activation at 500°C in the absence of air for both activated carbons was determined. The effect of pH, adsorbent dose, agitation speed, contact time and initial dye concentration on remazol blue (RB) adsorption were studied. Equilibrium data were fitted to Langmuir, Freundlich and Temkin isotherm models. The equilibrium data were best represented by the Langmuir isotherm model. The kinetic data were fitted to pseudo-first-order, pseudo-second-order, Elovich and intraparticle diffusion models, and it was found to follow closely the pseudo-second-order model.

Keywords: Adsorption; Isotherms; Kinetics; Reactive dye; Sawdust; Activated carbon

1. Introduction

There are various types of dyes such as acidic, reactive, disperse, metal complex, direct, sulphur, vat dye and so on. Nonetheless, the reactive type is the most popular utility in the textile industry and more than 15% of it runs off in wastewater stream [1]. A typical dye pollutant of textile wastewater, reactive brilliant blue X-BR (RBB X-BR), was investigated in this study. Synthetic dyes from the effluents of textile industry are known to be a major source of environmental pollution, in terms of both the volume of dye discharged and the effluent composition [2]. Approximately 1 million kg of dye are discharged in effluents from the textile industry each year in the world [3]. Reactive dyes have been a great concern for protecting the water ecosystem because many azo dyes and their breakdown products have been found toxic to aquatic life [4–9], mutagenic/carcinogenic [10] and gentoxic [11]. Recent studies indicate that approximately 12% of synthetic dyes are lost during manufacturing and processing operations and that 20% of the resultant color enter the environment through effluents from industrial wastewater treatment plants [12]. Color in dye house effluents has often been associated with the application of dyestuffs, during which up to 50% of the dyes may be lost to the effluent, which poses a major problem for the

* Corresponding author.

industry as well as a threat to the environment [13–16]. Decolorization of dye effluents has therefore acquired increasing attention during the last two decades. Several studies have been carried out for biological, physical and chemical treatment of dye containing effluents [17–19].

Among all methods of wastewater treatment, adsorption seems to offer the most considerable potential for the removal of dyes from industrial effluents [20]. The use of activated carbon in the adsorption process of dyes as well as inorganic pollutants from wastewater has many advantages such as high surface area, unique chemical nature of its surface and microporous structure [21]. On the other hand, the use of activated carbon has some disadvantages such as high cost together with the fact of difficult regeneration of it. In attempt to overcome this problem, many investigations are concerned with the use of inexpensive alternative materials as sources of activated carbon. Many source materials of agricultural origin have been used to produce activated carbon such as baggasse pith [22], sawdust [23], pandanus carbon [24] coconut shell [25] and many other agricultural wastes.

The aim of this investigation is to evaluate activated carbons derived from oak sawdust as a waste from wood manufacture in Egypt on the removal of reactive blue 19.

The activated carbons were produced by two different treatments. The two activated carbons characterized using FTIR, SEM and BET.

2. Materials and methods

2.1. Materials

Remazol brilliant blue (RB), an anionic dye is a G.R. product of ASMA Company, Egypt. It was used as received without further purification. The chemical structure and characterizations of the dye are presented in Fig. 1 and Table 1, respectively.

A stock solution of remazol blue (RB), (1000 mgL^{-1}) was prepared and suitably diluted to the required initial concentration. All chemicals were of analytical reagent grade.

2.2. Adsorbent preparation

Oak sawdust was washed with distilled water to remove the water-soluble impurities and surface adhered particles, dried in a digital dryer of (Carbolite, Aston lane, Hope Sheffield, 5302RP, England) for 24 h at 105°C to

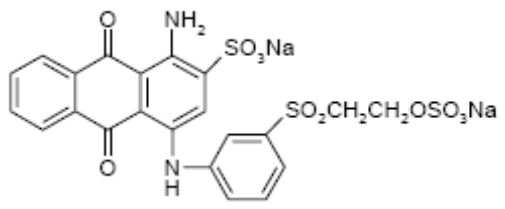

Fig. 1. Chemical structure of remazol brilliant blue (RB).

Table 1
Characterizations of the remazol brilliant blue (RB)

Parameters	Remazol brilliant blue (RB)
Color index name	Reactive blue 19
Chromophore group	Anthraquinone
Reactive anchor systems	Vinylsulfone
Molar mass, g/mol	506.5
Max absorbance, λm, nm	585
Purity, %	~50
Water solubility at 293 K, g/L	100
Acute oral toxicity LD50, mg/kg	2000
pH value, 10 g/L water	5–5.5

get rid of the moisture and other volatile impurities and sieved using sieve analyzer (AS200 Retsch, Germany) to different particle size ranges of 45–500 μm. The material after sieving in the range of 125–250 μm was isolated and divided into two parts and subjected by two different types of activation.

The first one was chemically treated followed by pyrolysis. The activation was carried out using 10% HNO_3 solution, where the sample was soaked in a ratio 1:10 w/v acid for 24 h with shaking at 200 rpm. After decantation, the sample was washed and dried at 105°C for 6 h. The dried sample was placed in a stainless steel covered tube and pyrolysed in a muffle furnace (Carbolite, Aston Lane, England) in the absence of air at 500°C for 1 h. Adsorbent obtained by chemical activation with 10% HNO_3 is termed Activated Carbon-1 (AC1).

The second one was physically activated by carbonization in a muffle furnace. The second part was placed in a stainless steel covered tube, where it was carbonized in the absence of air at 500°C for 1 h. Adsorbent obtained by physical activation only is termed Activated Carbon-2 (AC2).

2.3. Chemical and physical characteristics of adsorbent

The adsorbent was characterized with a number of methods. A scanning electron microscope (SEM) was used to examine the surface of the activated carbons using Jeol JSM-6360 LA analytical scanning electron microscope and the sample was prepared by coating with gold.

Also the textural characteristics of activated carbon including surface area, pore size analyzer (BET) were determined using standard N_2-adsorption techniques (Beckman Coulter, SA3100, USA) [26].

Surface chemistry of the activated carbons were determined using Fourier Transform Infrared spectrophotometer (FTIR) analysis was performed using FTIR-8400 S Shimadzu, Japan, prepared by mixing the samples with KBr.

The pH_{pzc} of carbons was determined using the pH drift method [27]. The pH_{pzc} is the pH on zero point charge, which is the point at which the net charge of the adsorbent is zero. The procedure of pH_{pzc} determination is described as follows: aliquots with 50 cm^3 of 0.01 M NaCl solution were prepared in different flasks. Their pH values were adjusted to the value between 2 and 12 with the addition of 0.01 M solutions of HCl or NaOH. When the pH value was constant, 0.15 g of activated carbon sample was added to each flask and it was shaken for 48 h. The final pH was measured using laboratory scale pH meter (PHS-3C Model) after 48 h. The pH_{pzc} value is the point where the curve pH_{final} vs. $pH_{initial}$ crosses the line $pH_{initial} = pH_{final}$ [28].

2.4. Adsorption study

Adsorption experiments with AC1 and AC2 were performed by batch technique at room temperature (22±2°C). A series of 250-mL Erlenmeyer flasks containing 100 mL of RB solutions of various concentrations (10–200 mg/L) and required doses of adsorbents (0.5–10 g/L) were employed at a desired pH by adding a required amount of 0.1 M HCl or 0.1 M NaOH solutions. These flasks were shaken using an orbital shaker (Yellow line Os10 Control, Germany) for a specific period of contact time (2–330 min) to achieve equilibration. Once the equilibrium was reached, the solution was carefully filtered and concentration of the dye in the solution after equilibrium adsorption was determined by measuring the absorbance. The effects of the medium pH on the adsorption capacities of AC1 and AC2 were investigated in the pH range 1.0–12.0. In adsorption batch experiments, the pH of each solution was measured by using a laboratory scale pH meter (PHS-3C Model).

2.5. Dye analysis

The concentration of RB remaining in the supernatant after and before adsorption was determined with a 1.0 cm light path quartz cells using UV-Vis double beam spectrophotometer (LABOMED, Inc.) at λ_{max} of 585 nm.

The adsorbed dye amount (mg/g), q_t and the percentage removal of dye at any time were computed as follows, respectively:

$$q_t = (C_0 - C_t) \cdot (V / M) \quad (1)$$

$$\% \text{ removal } = \left[(C_0 - C_t) / C_0 \right] \cdot 100 \quad (2)$$

where C_0 and C_t are the initial and any time t dye concentration (mg/L), V is the solution volume (L) and M is the adsorbent mass (g).

3. Results and discussion

3.1. Chemical and physical characteristics of adsorbent

3.1.1. Scanning electron microscope

Scanning electron microscope technique (SEM) was employed to observe the surface physical morphologies of active carbon produced by acid treatment as well as heat treatment of oak sawdust. The SEM of AC1 was produced from treatment with nitric acid and AC2 was produced from pyrolysis of oak sawdust. Fig. 2.shows that AC1 has honey comb void. It was obvious that the nitric acid treated active carbon AC1 was full of cavities, showed a larger interior pore and it could be explained by the solublization of some ingredients of the walls by nitric acid treatment. On the other hand, the active carbon produced from pyrolysis of sawdust AC2 showed

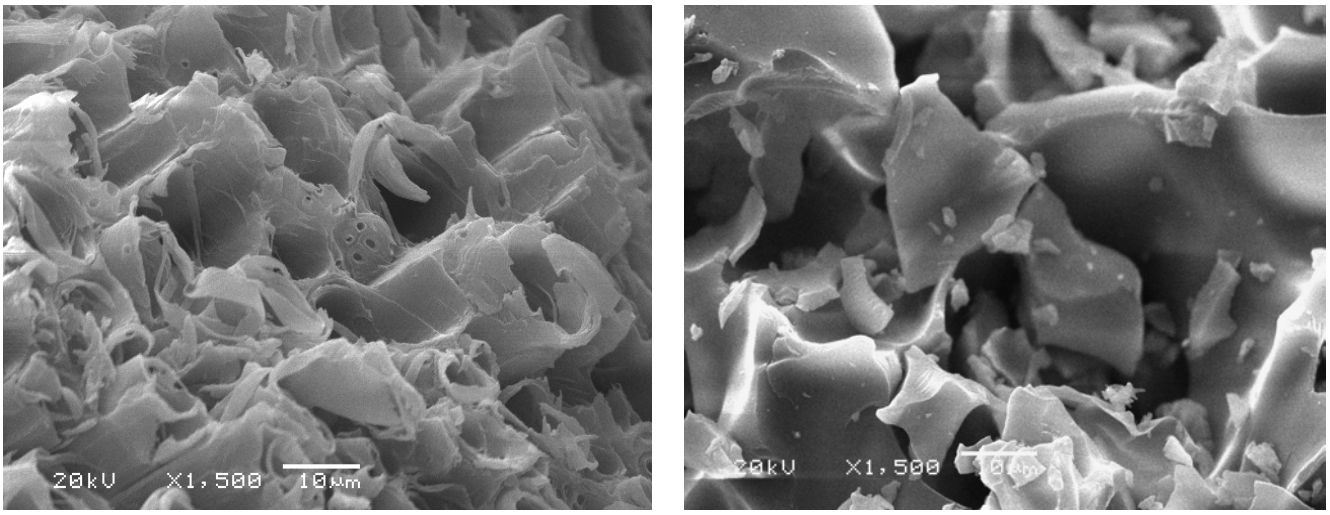

(a) (b)

Fig. 2. Scanning electron micrograph of (a) AC1 and (b) AC2.

fractured and fragmented structure more than AC1. The carbon had a sponge-like structure [29].

3.1.2. Surface area, pore size analyzer (BET)

The preparation of activated carbon by activation removes non-carbon elements such as hydrogen and oxygen, and leads to a carbon skeleton (char), with a rudimentary pore structure. Meanwhile in case of chemical activation the main role of the activating compound is the degradation of cellulosic materials. This is achieved upon thermal treatment, where the final pore structure is formed. On one hand, it leads to hydrolysis of lignocellulosic materials and subsequent partial extraction of some products, thus weakening the particle which swells. On the other hand, it occupies a volume which inhibits the contraction of the particle during the heat treatment, thus leaving porous structure. So Activated carbon from thermal activation AC2 shows BET surface area 140.9 m^2/g which is much lower than that of the chemically treated activated carbon AC1 with BET surface area 276.64 m^2/g.

3.1.3. Infrared spectra

The FTIR results are shown in Fig. 3. Peaks around 1700 cm^{-1} appear in both active carbon AC1 and AC2 and they could be attributed to the carbonyl group of the carboxylic acid group. Also a peak appearing in the acid treatment active carbon as well as heat treated active carbon at 1600 cm^{-1} could be assigned as C–C quinines or the presence of carbonates or carboxyl carbonate. There is a significant peak in nitric acid treated active carbon AC1 at 2355 cm^{-1} which may be attributed to nitriles or nitrogen double bond of thiol or thiol substituted compounds. In the case of heat treated active carbon AC2 there are two peaks at 1255 cm^{-1} and 1422 cm^{-1} which may be assigned to C–O–H bending or C–O ether and –C=C– cyclic amide respectively. The region around 3000 cm^{-1} showed a very broad peak due to the stretching vibration of surface hydroxyl groups with the hydroxyl groups of water adsorbed molecules.

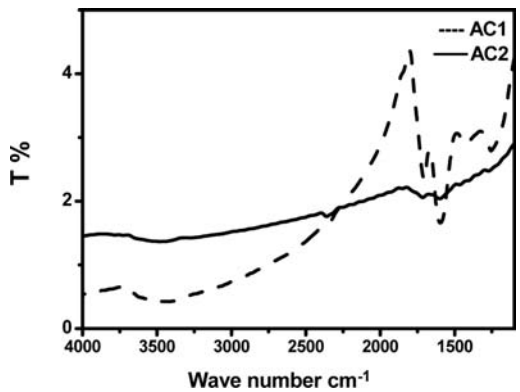

Fig. 3. FTIR spectra of AC1andAC2.

3.1.4. Zero charge point of PH

Point of zero charge (pH_{pzc}) is an important characteristics for any activated carbon as they indicate the acidity/basicity of the adsorbent, type of activated carbon (either H- or L-type), and the net surface charge of the carbon in the solution.

The combined influence of all the functional groups of activated carbon determines pH_{pzc}, i.e., the pH at which the net surface charge on carbon was zero. At $pH < pH_{pzc}$, the carbon surface has a net positive charge, while at $pH > pH_{pzc}$ the surface has a net negative charge [30]. The pH_{pzc} of theAC1 was 3.4 and the pH_{pzc} of the AC2 was 8.2.

3.2. Determination of optimum adsorption conditions

In order to determine the optimum operational parameters governing the adsorption process, the effect of pH, adsorbent dose, contact time, initial dye concentration and agitation speed were investigated.

3.2.1. Effect of initial pH

Solution pH affects both aqueous chemistry and surface binding sites of the adsorbents. The effect of initial pH on adsorption of RB was studied from pH 1 to 12 at 22±2°C, constant initial dye concentration of 50 mg. L^{-1}, adsorbent dose of 10 g L^{-1}, agitation speed 200 rpm and contact time of 2 h. Fig. 4. shows the effect of pH on the percentage removal of RB dye onto AC1 and AC2. The maximum removal of the RB dye for both AC1 and AC2 is obtained at studied pH 1. Fig. 4. depicts that the pH significantly affects the extent of adsorption of dye over the AC1 and AC2, and a reduction in the removal with increasing pH was observed. The hydrolysis constant value of the sulfonate groups of the dye molecule is 2.1 [31]. This functional group can be easily dissociated and thus, the dye molecule has net negative charges in the working experimental conditions. In this pH range the

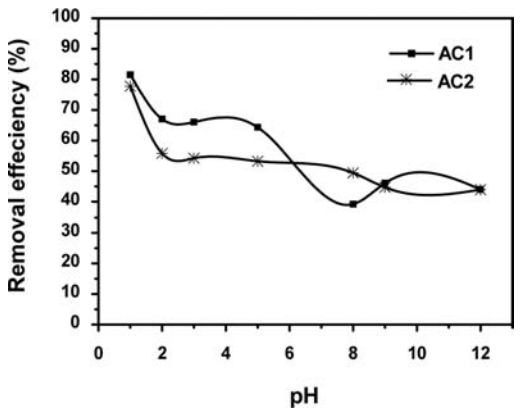

Fig. 4. Effect of pH on the removal efficiency of RB dye by AC1 and AC2. (Initial dyes concentration 50 mg.L^{-1}, adsorbent dose 10 g L^{-1}, agitation speed 200 rpm, temperature 22±2°C and contact time 2 h.)

surface of AC1 and AC2 are positively charged (pH_{pzc} for AC1 = 3.4 and AC2 = 8.2).

Higher uptakes of dye obtained at lower pH values may be due to the electrostatic attractions between these negatively charged dye's anions and positively charged adsorbent's surface (AC1 and AC2) [32]. A lower adsorption at higher pH values may be due to the abundance of OH^- ions and because of ionic repulsion between the negatively charged surface and the anionic dye molecules. There are also no more exchangeable anions on the outer surface of the adsorbents at higher pH values and consequently the adsorption decreases [33–35]. Similar results were reported for the adsorption of other reactive dyes from aqueous solutions [36,37].

Also, it was observed that at constant pH the percent removal increased in the order AC1 > AC2, and this means that the chemically treated adsorbent is favorable for anionic dye removal.

Due to the higher pH_{pzc} of AC2 than that of AC1, AC2 showed higher efficiency than AC1 in the pH range from 6.5 to 8 resulted from the presence of positive charge on its surface below pH_{pzc}.

3.2.2. Effect of the adsorbent dose

The effect of the adsorbent dose (AC1 and AC2) on the adsorption of RB was investigated with different adsorbent doses in the range of 0.5–10 g/L at a temperature 22±2°C, initial pH 1, initial dye concentration 50 mg/L, agitation speed 200 rpm and contact time 2 h.

Fig. 5 shows the effect of the adsorbent dose (AC1 and AC2) on the percentage removal of RB and the uptake capacity of AC1 and AC2. It was observed that the percentage removal of RB increased with increasing the adsorbent dose for both AC1 and AC2. This may be attributed to the increase of the adsorbent surface area and availability of more adsorption sites resulting from the increased dose of the adsorbent. While the adsorbed amounts of RB per unit adsorbent weight decreased by increasing the adsorbent dose from 0.5 to 10 g/L. At higher adsorbent (AC1 and AC2) to solute concentration ratios, there is a very fast superficial sorption onto the adsorbent surface that produces a lower solute concentration in the solution than when the adsorbent to solute concentration ratio is lower [38]. The increase in the adsorbed RB amounts per unit adsorbent weight at a low adsorbent dose can be explained by the availability of more adsorption sites. The decrease in the uptake amounts (q, mg/g) may be due to the splitting effect of flux (concentration gradient) between adsorbate and adsorbent with the increasing adsorbent dose causing a decrease in the amount of dye adsorbed onto the unit weight of the adsorbent [38].

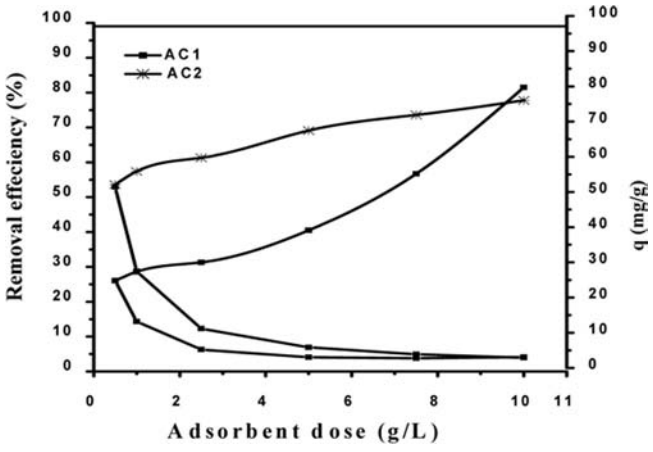

Fig. 5. Effect of adsorbent dose on the adsorption of RB dye by AC1 and AC2. (Initial dye concentration 50 $mg.L^{-1}$, pH = 1, agitation speed 200 rpm, temperature 22±2°C and contact time 2 h.)

Another reason may be due to the particle interactive behavior, such as aggregation, resulting from the high adsorbent dose. Such aggregation would lead to a decrease in the total surface area of the adsorbent and an increase in the diffusion path length. Similar phenomena were also observed for malachite green adsorption on sawdust [39] and reactive dyes onto the cross-linked chitosan beads [35].

3.2.3. Effect of contact time and initial dye concentration

The effect of contact time on the percentage removal of RB dye by AC1 and AC2 is shown in Fig. 6. The removal increases with time and attains equilibrium in 180 min for all concentrations studied (10–200 mg/L) and did not depend on the initial dye concentrations. The curves were single, smooth and continuous till the saturation of dye on the AC1 and AC2 surface. Similar results were reported for various dye adsorptions by other adsorbents [40–42]. Equilibrium time is one of the important considerations in the design of water and wastewater treatment systems because it influences the size of the reactor, thereby the plant economics [43].

The rate of percent dye removal is higher in the beginning due to a larger surface area of the adsorbent being available for the adsorption of the dye. After adsorption, the rate of dye transported from the exterior to the interior sites of the adsorbent particles. The two stage sorption mechanism with the first rapid and quantitatively predominant and the second slower and quantitatively insignificant has been extensively reported in literature [44].

The initial concentration provides an important driving force to overcome all mass transfer resistances of all molecules between the aqueous and solid phases [45].

Also from Fig. 6 it can be noticed that by increasing the initial dye concentration the percentage removal decreased, this indicates that there was a reduction in immediate solute adsorption, owing to the lack of available active sites required for the high initial concentration of RB, while the actual amount of dye adsorbed per unit

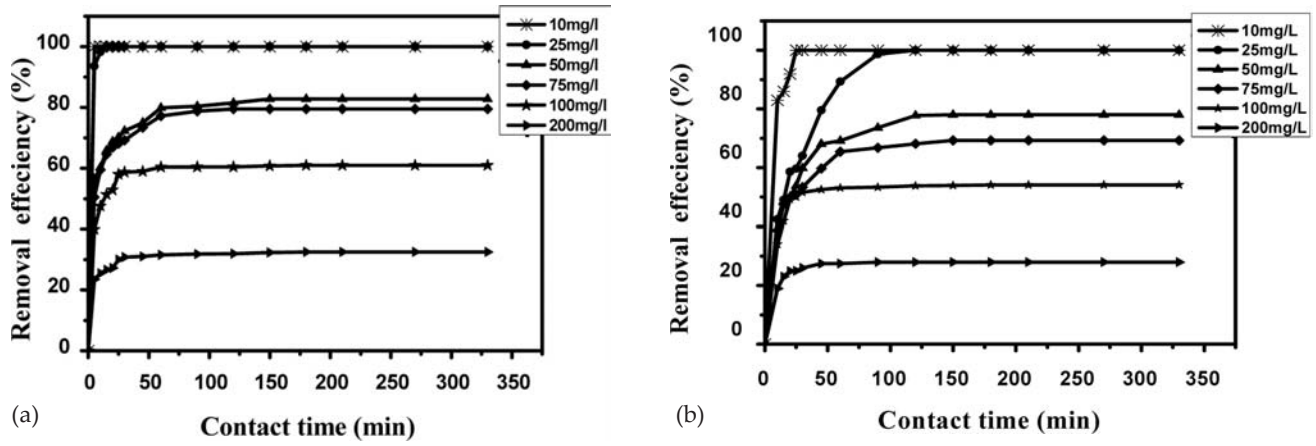

Fig. 6. Effect of contact time on the removal efficiency of RB dye by a) AC1 and b) AC2. (pH = 1, agitation speed 200 rpm , temperature 22±2°C and adsorbent dose 10 g L^{-1}.)

mass of activated carbon increased with the increased in initial concentration as presented in Fig. 7. This increase is due to the decrease in resistance to the uptake of solute from dye solution. Similar results have been reported in literature [46,47].

Finally, it can be noticed from Fig. 6 that AC1 has the maximum percentage removal compared to AC2.

3.2.4. Effect of agitation speed

Agitation is an important parameter in sorption phenomena, influencing the distribution of the solute in the bulk solution and the formation of the external boundary film. The effect of agitation speed (in rpm) on the % removal of the original dye concentration was investigated in the range of 0–400 rpm of the agitation speed while the temperature, initial pH, adsorbent dose, initial dye concentration and contact time values were kept at 22±2°C, 1,10 g/L ,50 mg/L and 2 h, respectively, as shown in Fig. 8. The % removal seemed to be affected by the agitation speed for values between 0 and 200 rpm, thus confirming that the influence of external diffusion on the sorption kinetic control plays a significant role. Also it is clear that while increasing the mixing rate from 200 to 400 rpm, % removal decreased from 81.5 to 61.2 and 77.8 to 32.4 for AC1 and AC2, respectively. This decrease may be attributed to an increase in desorption tendency of dye molecules and/or having similar speed of adsorbent particles and adsorbate ions (i.e., the formation of a more stable film around the adsorbent particles). This

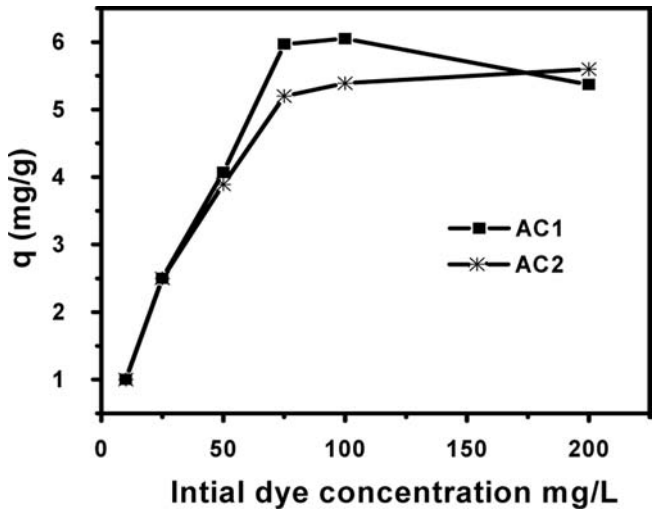

Fig. 7. Effect of initial dye concentration on the adsorbed amount/g of RB dye by AC1 and AC2. (Adsorbent dose 10 g/L, pH = 1, agitation speed 200 rpm, temperature 22±2°C and contact time 2 h.)

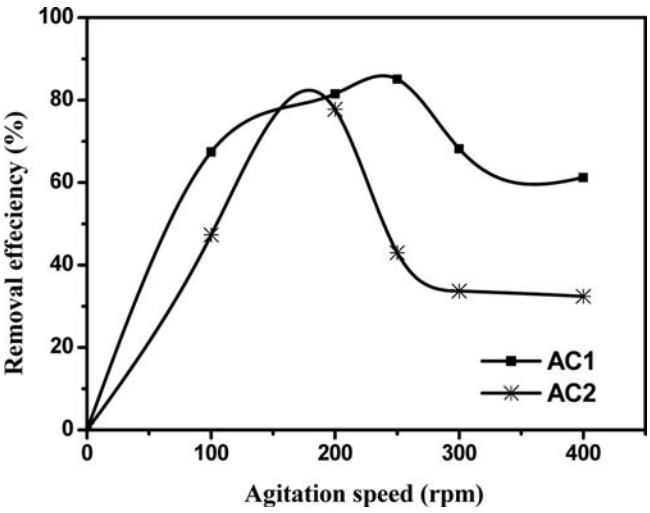

Fig. 8. Effect of agitation speed on the removal efficiency of RB dye by AC1 and AC2. (Initial dyes concentration 50 mg.L^{-1}, pH = 1, adsorbent dose 10 g/L, temperature 22±2°C and contact time 2 h.)

also indicates that a 200 rpm shaking rate is sufficient to assure that all the surface binding sites are made readily available for dye uptake. Then the effect of external film diffusion on the adsorption rate can be assumed to be insignificant. The results were in agreement with Batzias and Sidiras [48].

All adsorption parameters were studied in accordance with the characterization results of AC1 and AC2, where AC1 gives higher efficiency than AC2, which could be attributed to the pores widening. It results from the treatment and the solvolysis of the constituent of the boundary walls.

3.3. Adsorption isotherms

The adsorption isotherm indicates how the adsorption molecules are distributed between the liquid phase and the solid phase when the adsorption process reaches an equilibrium state. The analysis of the isotherm data by fitting them to different isotherm models is an important step to find a suitable model that can be used for design purposes [49]. Adsorption isotherm is basically important to describe how solutes interact with adsorbents, and is critical in optimizing the use of adsorbents. Adsorption isotherm study was carried out on three isotherm models: the Langmuir, Freundlich and Temkin isotherm models. The applicability of the isotherm equation to the adsorption study done was compared by judging the correlation coefficients, R^2.

3.3.1. Langmuir adsorption model

The Langmuir isotherm assumes monolayer adsorption onto a surface containing a finite number of adsorption sites of uniform strategies of adsorption with no transmigration of adsorbate in the plane of the surface [50]. The linear form of the Langmuir isotherm equation is given as:

$$c_e / q_e = 1/(Q_0 b) + C_e / Q_0 \quad (3)$$

where C_e is the equilibrium concentration of the adsorbate (mg/L), q_e is the equilibrium amount of adsorbate adsorbed per unit mass of adsorbent (mg/g), Q_0 and b are Langmuir constants and are the significance of the maximum adsorption capacity corresponding to complete monolayer coverage (mg of adsorbate per g of adsorbent) and energy of adsorption (L/mg), respectively.

When C_e/q_e was plotted against C_e, a straight line with the slope of $1/Q_0$ and intercept of $1/(Q_0 b)$ was obtained (figure is not included). The values of Langmuir constants b and Q_0 are listed in Table 2 along with the corresponding correlation coefficient. The correlation coefficient R^2 of 0.99 for both AC1 and AC2 indicated that the adsorption data of RB on the AC1 and AC2 were well fitted to the Langmuir isotherm. The essential characteristics of the Langmuir isotherm can be expressed in terms of a dimensionless equilibrium parameter (R_L) [50]. The parameter is defined by:

$$R_L = 1/(1 + b/C_0) \quad (4)$$

where b is the Langmuir constant and C_0 is the initial dye concentration (mg/L). The value of R_L indicates the type of the isotherm to be either unfavorable ($R_L > 1$), linear ($R_L = 1$), favorable ($0 < R_L < 1$) or irreversible ($R_L = 0$). All the values of R_L for both AC1 and AC2 are listed in Table 3 and are observed to be in the range 0–1, confirming that the Langmuir isotherm was favorable for adsorption of RB onto the AC1 and AC2 under the conditions used in this study.

3.3.2. Freundlich model

Freundlich adsorption isotherm is an indicator of the extent of heterogeneity of the adsorbent surface [50]. The Freundlich adsorption model stipulates that the ratio of solute adsorbed to the solute concentration is a function of the solution. The well-known logarithmic form of the Freundlich isotherm is given by the following equation:

$$\log q_e = \log K_f + 1/n \log c_e \quad (5)$$

where K_f is a constant for the system, related to the bonding energy. K_f can be defined as the adsorption or distribution coefficient and respects the quantity of dye adsorbed onto adsorbents for a unit equilibrium concentration (a measure of adsorption capacity, mg g^{-1}). A plot of log (q_e) vs. log (c_e), where the values of K_f and $1/n$ are determined from the intercept and slope of the linear regressions (figure is not included), are listed in Table 2 along with the corresponding correlation coefficient for AC1 and AC2. The slope of $1/n$ ranging between 0 and 1 for both AC1 and AC2 is a measure of the adsorption intensity or surface heterogeneity, becoming more heterogeneous as

Table 2
Langmuir, Freundlich and Temkin adsorption constants for different adsorbent material

Type of adsorbent	Langmuir			Freundlish			Temkin		
	Q_0	b	R^2	K_f	$1/n$	R^2	a	b	R^2
AC1	6.62	0.293	0.999	3.64	0.13	0.60	–1.91	0.93	0.64
AC2	5.76	0.276	0.999	3.17	0.126	0.69	–2.53	1.22	0.72

Table 3
R_L values for different adsorbents

Dye concentration (mg/l)	Value of R_L	
	AC1	AC2
50	0.064	0.068
75	0.044	0.046
100	0.033	0.035
200	0.017	0.018

its value gets closer to zero [51]. A value for 1/*n* below 1 indicates a normal Freundlich isotherm while 1/*n* above 1 is indicative of cooperative adsorption [52]. The low values of R^2 (<< 90%) for AC1 and AC2 show that the adsorption of RB dye on the different adsorbents used could not be well described by the Freundlich isotherms.

3.3.3. Temkin model

Temkin and Pyzhev considered the effects of indirect adsorbent/adsorbate interactions on the adsorption isotherm. The heat of adsorption of all the molecules in the layer would decrease linearly with coverage due to adsorbent/adsorbate interactions [53]. The Temkin isotherm has been used in the following form:

$$q_e = a + b \ln C_e \tag{6}$$

Therefore a plot of q_e vs. ln C_e enables one to determine the constants *a* and *b* from the slope and intercept (figure is not included). When *a* value is larger, this means that the adsorbent/adsorbate interaction is also larger [54]. The constants *a* and *b* together with the R^2 values are listed in Table 2. The low values of R^2 (<< 90%) for AC1 and AC2 show that the adsorption of RB dye on the different adsorbents used could not be well described by the Temkin isotherm.

Finally, the applicability of the three isotherm's models (Langmuir, Temkin and Freundlich) for the present data approximately follows the Langmuir isotherm in the case of RB dye on AC1 and AC2.

3.4. Sorption dynamics

The study of adsorption dynamics describes the solute uptake rate and evidently this rate controls the residence time of adsorbate uptake at the solid–solution interface. The kinetics of RB adsorption on AC1 and AC2 was analyzed using pseudo first order, pseudo second order, Elovich and intraparticle diffusion kinetic models. The conformity between the experimental data and the model predicted values was expressed by the correlation coefficients (R^2 values close or equal to 1). A relatively high R^2 value and indicates that the model successfully describes the kinetics of the adsorption.

3.4.1. Pseudo-first-order model

The pseudo-first-order model was presented by Lagergren [55]. The Lagergren's first-order reaction model is expressed as follows by Yalçın et al. [56]:

$$dq_t / d_t = k_1 \left(q_e - q_t \right) \tag{7}$$

where q_e and q_t are the amounts of dye (mg/g) adsorbed on the adsorbent at equilibrium, and at time *t*, respectively and k_1 is the first-order reaction rate constant (min^{-1}). Integrating and applying the boundary condition, $t = 0$ and $q_t = 0$ to $t = t$ and $q_t = q_t$, Eq. (7) takes the form:

$$\ln\left(q_e - q_t \right) = \ln q_e - k_1 t \tag{8}$$

The values of ln ($q_e - q_t$) were linearly correlated with *t* (figures are not included). The values of k_1 and q_e were determined from the slope and intercept of the linear plots ln ($q_e - q_t$) against t respectively for the adsorption of RB using AC1 and AC2 and are listed in Table 4 along with the corresponding correlation coefficients. The correlation coefficients for the first-order model are low for all adsorbents and concentrations. Also, the estimated values of q_e calculated from the equation differed from the experimental values (Table 4). Therefore it can be inferred that the first-order model does not show good compliance with experimental data.

3.4.2. Pseudo-second-order model

The sorption data was also analyzed in terms of the pseudo second-order mechanism described by [57–61]

$$dq_t / dt = k_2 \left(q_e - q_t \right)^2 \tag{9}$$

where k_2 is the rate constant of the pseudo-second-order sorption (g/mg min). Integrating and applying boundary conditions $t = 0$ and $q_t = 0$ to $t = t$ and $q_t = q_t$, Eq. (9) becomes

$$1/\left(q_e - q_t \right) = 1/q_e + k_2 t \tag{10}$$

This is the integrated rate law for a pseudo second order reaction. Eq. (10) can be rearranged to obtain Eq. (11), which has a linear form:

$$t/q_t = 1/k_2 q_e^2 + 1/q_e \,(t) \tag{11}$$

The values of k_2 and qe were determined from the intercept and slope of the linear plots ln ($q_e - q_t$) against *t* respectively for the adsorption of RB using AC1 and AC2 (figures are not included) and are listed in Table 4 along with the corresponding correlation coefficients. Also the estimated values of q_e calculated from Eq. (11) are listed in Table 4. The correlation coefficients R^2 for the pseudo-second-order adsorption model have the highest values (> 0.99), suggesting that the dye adsorption process is predominant by the pseudo-second-order adsorption mechanism.

Table 4
Comparison of the first- and second-order adsorption rate constants, calculated and experimental q_e values for different adsorbents

Type of adsorbent	Dye concentration (mg/l)	$q_{e\,exp}$	1st order			2nd order		
			R^2	k_1	$q_{e\,calc}$	R^2	k_2	$q_{e\,calc}$
AC1	50	4.14	0.827	0.027	1.16	0.9998	0.054	4.23
	75	5.97	0.99	0.043	2.68	0.9999	0.041	6.11
	100	6.1	0.87	0.037	0.66	0.9998	0.0713	6.18
	200	6.5	0.605	0.03	1.63	0.9998	0.057	6.58
AC2	50	3.9	0.91	0.04	3.13	0.9989	0.025	4.11
	75	5.2	0.95	0.043	3.07	0.9995	0.032	5.38
	100	5.41	0.83	0.042	1.32	0.9999	0.095	5.47
	200	5.6	0.89	0.088	3.09	0.9958	0.469	5.65

3.4.3. Elovich equation

The applicability of the Elovich equation to the sorption process was also tested. The simple Elovich model may be expressed in the form [62,63]:

$$q_t = A + B\ln t \quad (12)$$

where A represents the rate of chemisorptions at zero coverage (mg/g min) and B is related to the extent of the surface coverage and activation energy for chemisorptions (g/mg).

Thus, a plot of q_t vs. ln t should yield a linear relationship with a slope of B and an intercept of A, if the sorption process fits the Elovich equation.

The Elovich equation parameters A, B and the correlation coefficients, R^2 for the sorption of the RB using AC1 and AC2 (figures are not included) are listed in Table 5. The R^2 values are not high and show not good fit. Thus, the Elovich equation could not be a good model for the sorption process.

Comparison of the three models reveals that the R^2 for first-order, pseudo-second-order and the Elovich equations show that the results can be well represented by the pseudo-second-order model.

Hence, on the basis of the excellent fit of the pseudo-second order and the correlation of the experimental results with the pseudo-second-order model, the main adsorption mechanism is probably chemisorption reaction.

3.4.4. Intraparticle diffusion model

Intraparticle diffusion can be described by three consecutive steps [64]:

(i) The transport of sorbate from bulk solution to outer surface of the sorbent by molecular diffusion, known as external (or) film diffusion.
(ii) Internal diffusion, the transport of sorbate from the particles surface into interior sites.
(iii) The sorption of the solute particles from the active sites into the interior surface of the pores.

The overall rate of the sorption process will be controlled by the slowest, the rate limiting step. The nature of the rate-limiting step in a batch system can be determined

Table 5
Elovich adsorption rate constants and calculated and experimental q_e values for different adsorbents

Type of adsorbent	Dye concentration (mg/l)	$q_{e\,exp}$	Elovich			
			R^2	A	B	$q_{e\,calc}$
AC1	50	4.14	0.8674	42.51	2.564	30.97
	75	5.97	0.9604	80.99	4.703	59.825
	100	6.1	0.9482	10.27	7.539	67.345
	200	6.5	0.9487	11.53	9.723	67.782
AC2	50	3.9	0.8838	42.22	4.138	23.599
	75	5.2	0.8735	70.87	5.688	45.27
	100	5.41	0.94	85.27	8.003	49.259
	200	5.6	0.8428	105.5	12.61	48.738

from the properties of the solute and sorbent. In adsorption systems where there is the possibility of intraparticle diffusion being the rate-limiting step, the intraparticle diffusion approach described by Weber and Morris [65] is used. The rate constants, for intraparticle diffusion (k_i) are determined using equation given by Weber and Morris [65]. This equation can be described as [66–68]:

$$q_t = k_i t^{0.5} + c \quad (13)$$

where k_i and c are the intraparticle diffusion rate constants (mg/g min$^{0.5}$) under different initial concentrations of dye and a constant, respectively. In Figs. 9 and 10, respectively, plots of q_t (mg/g) vs. $t^{1/2}$ (min$^{-1/2}$) are presented for AC1 and AC2. The k_i is the slope of straight-line portions of the plot of q_t vs. $t^{0.5}$ and the value of c is the intercept. The values of constants k_i and c for intraparticle diffusion kinetics are given in Table 6. These plots have generally the double nature, i.e., the initial curve portions and final linear portions. It is explained by the fact that the initial curved portions are boundary layer diffusion effects. The final linear portions are a result of intraparticle diffusion effects. An extrapolation of the linear portions of the plots back to the axis yield intercepts (c) which are proportional to the extent of boundary layer thickness [69].

4. Conclusions

This study has demonstrated that activated carbons can be prepared from the chemical activation of oak sawdust with HNO_3 as activating agent followed by pyrolysis at 500°C in the absence of air and by physical activation at 500°C in the absence of air. The two activated carbons prepared from oak sawdust have been used as an adsorbent for the removal of RB from aqueous solutions. RB was found to adsorb stronger onto the surface of AC1 than onto that of AC2. Adsorption was influenced by various parameters such as initial pH, initial dye concentration, adsorbent dose and agitation speed. The maximum adsorption of RB dye by AC1 and AC2 occurred at an initial pH of 1.0. The removal efficiency increased with decreasing the dye concentration and increasing the dose of the adsorbent. Adsorption equilibrium data were fitted to the Langmuir, Freundlich and Temkin isotherms. The equilibrium data were well described by the Langmuir isotherm model, with the maximum monolayer adsorption.

It was found that the pseudo-second-order equation gave a better fit to the adsorption process than the pseudo-first-order equation and Elovich equation. Consequently, the main adsorption mechanism is probably a chemisorption reaction. Hence this model should be used in design applications. An intraparticle diffusion model developed by Weber and Morris was used to calculate the intraparticle diffusion coefficients. The adsorption data is properly controlled by both external mass transfer and intraparticle diffusion.

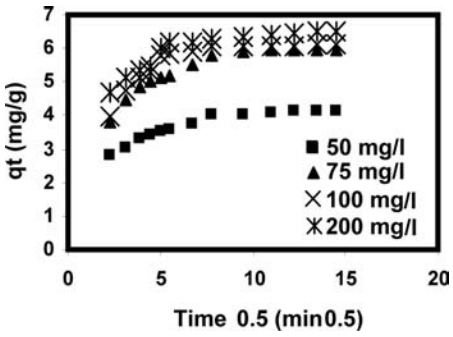

Fig. 9. Intraparticle diffusion plot for adsorption of RB dye by AC1.

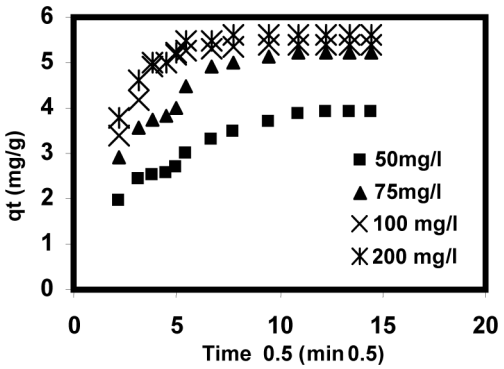

Fig. 10. Intraparticle diffusion plot for adsorption of RB dye by AC2.

Table 6
Intraparticle diffusion rate parameter at different initial dye concentration for different adsorbents

Dye concentration (mg/L)	Type of adsorbent					
	AC1			AC2		
	k_i	c	R^2	k_i	c	R^2
50	0.0247	3.802	0.88	0.0659	3.0324	0.78
75	0.0254	5.6391	0.73	0.0281	4.8307	0.76
100	0.0103	5.9516	0.88	0.0118	5.2531	0.85
200	0.0334	6.0291	0.95	00083	5.4966	0.39

Symbols

$1/n$ — Sorption intensity
A — Rate of chemisorptions at zero coverage, mg/g min
AC1 — Activated carbon prepared from oak sawdust by chemical activation
AC2 — Activated carbon prepared from oak sawdust by physical activation
B — Extent of the surface coverage and activation energy for chemisorptions, g/mg
b — Langmuir constant energy of adsorption, L/mg
BET — Surface area, pore size analyzer
C — Dye concentration at any time, mg/L
C_e — Equilibrium dye concentration, mg/L
C_0 — Initial dye concentration, mg/L
FTIR — Fourier transfer for infrared spectrophotometer
k_1 — First-order reaction rate constant, min^{-1}
k_2 — Second-order reaction rate equilibrium constant, g/mg min
K_f — Freundlich constant measure of adsorbent capacity, mg/g
k_i — Intraparticle diffusion rate constant, mg g^{-1} $min^{-1/2}$
M — Adsorbent mass, g
pH_{pzc} — pH on zero point charge
Q_0 — Langmuir constant adsorption capacity, mg/g
q_e — Amount of dye adsorbed at equilibrium, mg/g
q_t — Amount of dye adsorbed at any time, mg/g
R^2 — Correlation coefficient
RB — Remazol brilliant blue
R_L — Equilibrium parameter
SEM — Scanning electron microscope
t — Time, min
$t^{1/2}$ — Square root of time, $min^{1/2}$
V — Solution volume, L

References

[1] H. Park and W.Y. Choi, Visible light and Fe(III)-mediated degradation of acid orange in the absence of H_2O_2, J. Photochem. Photobiol. A: Chem., 159 (2003) 241–247.
[2] P.C. Vandevivere, R. Bianchi and W. Verstraete, Treatment and reuse of wastewater from the textile wet-processing industry: review of emerging technologies, J. Chem. Technol. Biotechnol., 72 (1998) 289–302.
[3] E.Y. Ozmen, S. Erdemir, M. Yilmaz and M. Bahadir, Removal of carcinogenic direct azo dyes from aqueous solutions using calix[n]arene derivatives, Clean, 35 (2007) 612–616.
[4] K.T. Chung, S.E.J. Stevens and C.E. Cerniglia, The reduction of azo dyes by the intestinal microflora, Crit. Rev. Microbiol., 18 (1992) 175–197.
[5] C. Wang, A. Yediler, D. Lienert, Z. Wang and A. Kettmp, Toxicity evaluation of reactive dyestuffs, auxiliaries and selected effluents in textile finishing industry to luminescent bacteria *Vibrio fischeri*, Chemosphere, 46 (2002) 339–344.
[6] C.Wang, A. Yediler, D. Lienert, Z.Wang and A. Kettrup, Ozonation of an azo dye C.I. Remazol Black 5 and toxicological assessment of its oxidation products, Chemosphere, 52 (2003) 1225–1232.
[7] Q. Tezcanli-Guyer and N.H. Ince, Degradation and toxicity reduction of textile dyestuff by ultrasound, Ulwas. Sonochem., 10 (2003) 235–240.
[8] F. Zhang, A. Yediler, X. Liang and A. Ketlrup, Effects of dye additives on the ozonation process and oxidation by-products: a comparative study using hydrolyzed C.I. Reactive Red 120, Dyes Pigments, 60 (2004) 1–7.
[9] S. Meriq, D. Kaptan and T. Olmez, Color and COD removal from wastewater containing Reactive Black 5 using Fenton's oxidation process, Chemosphere, 54 (2004) 435–441.
[10] K.T. Chung and S.E.J. Stevens, Degradation of azo dyes by environmental microorganisms and helmints, Environ. Toxicol. Chem., 12 (1993) 2121–2132.
[11] A. Gottlieb, C. Shaw, A. Smith, A. Wheatley and S. Forsythe, The toxicity of textile reactive azo dyes after hydrolysis and decolourisation, J. Biotechnol., 101 (2003) 49–56.
[12] A. Reife and H.S. Freemann, Environmental Chemistry of Dyes and Pigments, John Wiley and Sons Inc., Canada, 1996.
[13] H. Zollinger, in: H.F. Eblel and C.D. Brenzinger, eds., Colour Chemistry, 1st ed., VCH, New York, 1987, Chap. 16.
[14] C.E. Searle, Chemical Carcinogenesis, ACS Monograph, American Chemical Society, Washington, DC, 1976.
[15] M. Qamar, M. Saquib and M. Muneer, Semiconductor-mediated photocatalytic degradation of an azo dye, chrysoidine Y in aqueous suspensions, Desalination , 171 (2004) 185–193.
[16] J.J. Roxon, A.J. Ryan and S.E. Wright, Reduction of water-soluble azo dyes by intestinal bacteria, Food Cosmet. Toxicol., 5(3) (1967) 367–369.
[17] T. Robinson, G. McMullan, R. Marchant and P. Nigam, Remediation of dyes in textile effluent: a critical review on current treatment technologies with a proposed alternative, Bioresource Technol., 77 (2001) 247–255.
[18] S. Ledakowicz, M. Solecka and R. Zylla, Biodegradation, decolourisation and detoxification of textile wastewater enhanced by advanced oxidation processes, J. Biotechnol., 89 (2001) 175–184.
[19] D. Georgiou, P. Melidis, A. Aivasidis and K. Gimouhopoulos, Degradation of azo-reactive dyes by ultraviolet radiation in the presence of hydrogen peroxide, Dyes Pigments, 52 (2002) 69–78.
[20] K. Kadirvelu, M. Palanival, R. Kalpana and S. Rajeswari, Activated carbon from an agricultural by-product for the treatment of dyeing industry wastewater, Bioresource Technol., 74 (2000) 263–265.
[21] B. Toledo, J.R. Utrilla, M.A. Garcia and C.M. Castilla, Influence of the oxygen surface complexes of activated carbons on the adsorption of chromium ions from aqueous solutions: Effect of sodium chloride and humic acid, Carbon, 32 (1994) 93–100.
[22] N.K. Amin, Removal of reactive dye from aqueous solutions by adsorption onto activated carbons prepared from sugarcane bagasse pith, Desalination, 223 (2008) 152–161.
[23] S.E Abechi, C.E. Gimba, A. Uziaru and I.G. Ndukwe, Comparative studies on adsorption of methylene blue (MB) by sawdust and walnut shells carbon coated with ZnO, Sci. World J., 1 (2006) 33–35.
[24] R. Sudha, K. Kalapana, T. Rajachandrasekar and S. Arivoli, Comparative study on the adsorption kinetics and thermodynamics of metal ions onto acid activated low cost pandanus carbon, E-J. Chem., 4(2) (2007) 238–254.
[25] R.W. Gaikwad, Removal of Cd (II) from aqueous solution by activated charcoal derived from coconut shell, Electron. J. Environ. Agric. Food Chem., 3(4) (2004) 702–709.
[26] F. Guzel and Z. Tez, The characterization of the micropore structure of some activated carbon of plant origin by N_2 and CO_2 adsorption, Separ. Sci. Technol., 28 (1993)1609–1627.
[27] P. Faria, J. Orfao and M. Pereira, Adsorption of anionic and cationic dyes on activated carbons with different surface chemistries, Wat. Res., 38 (2004) 2043–2052.
[28] N. Wibowo, L. Setiyadhi, D. Wibowo, J. Setiawan and S. Ismadji, Adsorption of benzene and toluene from aqueous solutions onto

activated carbon and its acid and heat treated forms: Influence of surface chemistry on adsorption, J. Hazard. Mater., 146 (2007) 237–242.
[29] C. Namasivayam and D. Sangeetha, Recycling of agricultural solid waste, coirpith: removal of anions, heavy metals, organics and dyes from water by adsorption onto $ZnCl_2$ activated coirpith carbon, J. Hazard. Mater., B135 (2006) 449–452.
[30] Y. Al-Degs, M. Khraisheh, S. Allen and M. Ahmad, Effect of carbon on the removal of reactive dyes from textile effluent, Wat. Res., 34 (2000) 927–935.
[31] Y. Xue, H. Hou and S. Zhu, Removal of reactive dyes from aqueous solution by modified basic oxygen furnace slag: isotherm and kinetic study, Chem. Eng. J., 147(2–3) (2009) 272–279.
[32] B.H. Hameed, A.A. Ahmad and N. Aziz, Isotherms, kinetics and thermodynamics of acid dye adsorption on activated palm ash, Chem. Eng. J., 133 (2007) 195–203.
[33] P.K. Malik, Dye removal from wastewater using activated carbon developed from sawdust: adsorption equilibrium and kinetics, J. Hazard. Mater., B113 (2004) 81–88.
[34] G. Akkaya and A. Özer, Biosorption of acid red 274 (AR 274) on Dicranella varia: determination of equilibrium and kinetic model parameters, Process Biochem., 40 (2005) 3559–3568.
[35] M.S. Chiou, P.Y. Ho and H.Y. Li, Adsorption of anionic dyes in acid solutions using cross-linked chitosan beads, Dyes Pigments, 60 (2004) 69–84.
[36] M.S. Chiou and H.Y. Li, Equilibrium and kinetic modeling of adsorption of reactive dye on cross-linked chitosan beads, J. Hazard. Mater., B93 (2002) 233–248.
[37] A. Özcan and A. Safa Özcan, Adsorption of acid red 57 from aqueous solutions onto surfactant-modified sepiolite, J. Hazard. Mater., B 125 (2005) 252–259.
[38] V. Vadivelan and K.V. Kumar, Equilibrium, kinetics, mechanism, and process design for the sorption of methylene blue onto rice husk, J. Colloid Interface Sci., 286 (2005) 90–100.
[39] V.K. Garg, R. Gupta, A.B. Yadav and R. Kumar, Dye removal from aqueous solution by adsorption on treated sawdust, Bioresour. Technol., 89 (2003) 121–124.
[40] M.M. Abd El-Latif and A.M. Ibrahim, Adsorption, kinetic and equilibrium studies on removal of basic dye from aqueous solutions using hydrolyzed oak sawdust, Desal. Wat. Treat., 6 (2009) 252–268.
[41] C. Namasivayam and D. Kavitha, Removal of Congo red from water by adsorption onto activated carbon prepared from coir pith, Dyes Pigments, 54 (2002) 47–58.
[42] S.R. Sugunadevi, M.Sathishkumar, K. Shanthi, K. Kadirvelu and S. Pattabhi, Removal of direct T-blue R from aqueous solution onto carbonised sugarcane baggase waste, Indian J. Environ. Protect., 22 (2002) 500–505.
[43] K.K. Deepa, M. Sathishkumar, A.R. Binupriya, G.S Murugesan, K. Swaminathan and S.E. Yun, Sorption of Cr(VI) from dilute solutions and wastewater by live and pretreated biomass of *Aspergillus flavus*, Chemosphere, 62 (2006) 833–840.
[44] Y. Inbar, Y. Chen and Y. Hadar, Solid-state carbon-13 nuclear magnetic resonance and infrared spectroscopy of composted organic matter, Soil Sci. Soc. Am. J., 53(6) (1989) 1695–1701.
[45] G. Akkaya and A. Özer, Biosorption of acid red 274 (AR 274) on *Dicranella varia*: Determination of equilibrium and kinetic model parameters, Process Biochem., 40 (2005) 3559–3568.
[46] N. Kannan and M.M. Sundaram, Kinetics and mechanism of removal of methylene blue by adsorption on various carbons—A comparative study, Kinetics Dyes Pigments, 51 (2001) 25–40.
[47] F. Cicek, D. Ozer, A. Ozer and A. Ozer, Low cost removal of reactive dyes using wheat bran, J. Hazard. Mater., 146 (2007) 408–416.
[48] F.A. Batzias and D.K. Sidiras, Dye adsorption by prehydrolysed beech sawdust in batch and fixed-bed systems, Bioresour. Technol., 98 (2007) 1053–1062.
[49] M. El-Guendi, Homogeneous surface diffusion model of basic dyestuffs onto natural clay in batch adsorbers, Adsorpt. Sci. Technol., 8(2) (1991) 217–225.
[50] T.W. Weber and R.K. Chakkravorti, Pore and solid diffusion models for fixed-bed adsorbers, J. AIChE, 20 (1974) 228–233.
[51] F. Haghseresht and G. Lu, Adsorption characteristics of phenolic compound onto coal-reject-derived adsorbents, Energy Fuels, 12 (1998) 1100–1107.
[52] K. Fytianos, E. Voudrias and E. Kokkalis, Sorption–desorption behaviour of 2,4-dichlorophenol by marine sediments, Chemosphere, 40 (2000) 3–6.
[53] M. Hosseini, S.F.L. Mertens, M. Ghorbani and M.R. Arshadi, Asymmetrical schiff bases as inhibitors of mild steel corrosion in sulphuric acid media, Mater. Chem. Phys., 78 (2003) 800–808.
[54] S. Rengaraj, Y. Kim, C.K. Joo, K. Choi and J. Yi, Batch adsorptive removal of copper ions in aqueous solutions by ion exchange resins: 1200H and IRN97H, Korean, J. Chem. Eng., 21 (2004) 187–194.
[55] S. Lagergren, Zur theorie der sogenannten adsorption gel¨oster stoffe. Kungliga Svenska Vetenskapsakademiens, Handlingar, 24(4) (1898) 1–39.
[56] M. Yalçın, A. Gürses, C. Dögar and M. Sözbilir, The adsorption kinetics of cethyltrimethylammonium bromide (CTAB) onto powdered active carbon, Adsorption, 10 (2004) 339–348.
[57] R.L. Tseng, F.C. Wu and R.S. Juang, Liquid-phase adsorption of dyes and phenols using pinewood-based activated carbons, Carbon, 41 (2003) 487–495.
[58] Y.S. Ho and G. McKay, Sorption of dye from aqueous solution by peat, Chem. Eng. J., 70 (1998) 115–124.
[59] Y.S. Ho and G. McKay, Sorption of dyes and copper ions onto biosorbents, Process Biochem., 38 (2003) 1047–1061.
[60] Y.S. Ho and C.C. Chiang, Sorption studies of acid dye by mixed sorbents, Adsorption, 7 (2001) 139–147.
[61] F.C. Wu, R.L. Tseng and R.S. Juang, Adsorption of dyes and humic acid from water using chitosan-encapsulated activated carbon, J. Chem. Technol. Biotechnol., 77 (2002) 1269–1279.
[62] S.H. Chien and W.R. Clayton, Application of Elovich equation to the kinetics of phosphate release and sorption on soils, Soil Sci. Soc. Am. J., 44 (1980) 265–268.
[63] C.W. Cheung, J.E. Porter and G. McKay, Sorption kinetics for the removal of copper and zinc from effluents using bone char, Separ. Purif. Technol., 53 (2000) 55–64.
[64] M. Ügurlu, A. Gürses, C. Dögar and M. Yalçın, Removal of phenolic and lignin compounds from bleached kraft mill effluent by fly ash and sepiolite, Adsorption 11 (2005) 87–97.
[65] W.J. Weber and J.C. Morris, Kinetics of adsorption on carbon from solution, J. Sanit. Eng. Div. Am. Soc. Civ. Eng., 89 (1963) 31–60.
[66] C.K. Jain and M.K. Sharma, Adsorption of cadmium on bed sediments of River Hindon: Adsorption models and kinetics, Water Air Soil Pollut., 137 (2002) 1–19.
[67] M. Basibuyuk and C.F. Forster, An examination of the adsorption characteristics of a basic dye (Maxilon Red Bl-N) on to live activated sludge system, Process Biochem., 38 (2003) 1311–1316.
[68] R. Sivaraj, C. Namasivayam and K. Kadirvelu, Orange peel as an adsorbent in the removal of acid Violet 17 (acid dye) from aqueous solutions, Waste Manage., 21 (2001) 105–110.
[69] L. Markovska, V. Meshko, V. Noveski and M. Marinovski, Solid diffusion control of the adsorption of basic dyes onto granular activated carbon and natural zeolite in fixed bed columns, J. Serbian Chem. Soc., 66 (2001) 463–475.